

Exchange anisotropy, disorder, and frustration in diluted, predominantly ferromagnetic, Heisenberg spin systems

Chenggang Zhou,¹ Malcolm P. Kennett,² Xin Wan,^{3,*} Mona Berciu,⁴ and R. N. Bhatt¹

¹*Department of Electrical Engineering, Princeton University, Princeton, New Jersey 08544, USA*

²*TCM Group, Cavendish Laboratories, Cambridge University, Madingley Road, Cambridge CB3 0HE, United Kingdom*

³*National High Magnetic Field Laboratory, Florida State University, Tallahassee, Florida 32310, USA*

⁴*Department of Physics and Astronomy, University of British Columbia, Vancouver, Canada BC V6T 1Z1*

(Received 14 October 2003; revised manuscript received 10 February 2004; published 19 April 2004)

Motivated by the recent suggestion of anisotropic effective exchange interactions between Mn spins in $\text{Ga}_{1-x}\text{Mn}_x\text{As}$ (arising as a result of spin-orbit coupling), we study their effects in diluted Heisenberg spin systems. We perform Monte Carlo simulations on several phenomenological model spin Hamiltonians, and investigate the extent to which frustration induced by anisotropic exchanges can reduce the low-temperature magnetization in these models and the interplay of this effect with disorder in the exchange. In a model with low coordination number and purely ferromagnetic exchanges, we find that the low-temperature magnetization is gradually reduced as exchange anisotropy is turned on. As the connectivity of the model is increased, the effect of small-to-moderate anisotropy is suppressed, and the magnetization regains its maximum saturation value at low temperatures unless the distribution of exchanges is very wide. To obtain significant suppression of the low-temperature magnetization in a model with high connectivity, as is found for long-range interactions, we find it necessary to have both ferromagnetic and antiferromagnetic exchanges (e.g., as in the Ruderman-Kittel-Kasuya-Yosida interaction). This implies that disorder in the sign of the exchange interaction is much more effective in suppressing magnetization at low temperatures than exchange anisotropy.

DOI: 10.1103/PhysRevB.69.144419

PACS number(s): 75.10.Nr, 75.10.Hk, 02.70.Tt, 75.60.-d

I. INTRODUCTION

It has recently been suggested that frustration effects may be important for the magnetic properties of diluted magnetic semiconductors (DMS's) such as $\text{Ga}_{1-x}\text{Mn}_x\text{As}$.¹⁻³ The reported Curie temperatures (T_c) in these compounds continue to rise, with a maximum of 140 K recently reported for $\text{Ga}_{1-x}\text{Mn}_x\text{As}$,⁴ and even higher values reported for related materials.⁵ Aside from increasing T_c , it will also be important to have a thorough understanding of the different aspects of their magnetic properties over a wide temperature range in order to be able to design optimized spintronic devices. In theoretical analyses, Zarand and Janko¹ showed that within the Ruderman-Kittel-Kasuya-Yosida (RKKY) approximation, a proper treatment of the spin-orbit coupling leads to anisotropic exchanges between Mn spins. Using this interaction they found that the saturation magnetization is reduced by up to 50% at low temperatures. Experimentally it has been observed that in many DMS, the saturation magnetization at low temperatures is not as large as would be expected if all Mn moments were aligned (i.e., the full saturation value).⁶ While it is likely that magnetically inactive Mn, such as Mn interstitials,⁷ may account for some of the suppression of the low-temperature magnetization, the results of Zarand and Janko suggest that anisotropic spin interactions may also play a significant role in accounting for it. We carefully investigate this possibility in this paper.

In a system consisting of localized spins (local moments) coupled to noninteracting fermions (carriers), where the spin-carrier interaction is a perturbation on the fermionic Hamiltonian, low-lying spin excitations can be described in terms of RKKY interactions between the spins. In DMS's, the car-

rier density is low (lower than the density of local moments by a considerable factor, due to carrier compensation), and the carrier-spin interaction is quite strong (necessary to enable a high T_c). Consequently, the RKKY approximation appears unlikely to be appropriate for a *quantitative* description of the ferromagnetism in $\text{Ga}_{1-x}\text{Mn}_x\text{As}$ since the Fermi energy is not necessarily much larger than the magnetic coupling. However, the qualitative prediction of anisotropic exchange may be present in more precise treatments.⁸

In what follows, therefore, we assume that the magnetic properties of the system can be modeled in terms of an effective spin Hamiltonian, with a form that maintains the symmetry properties of the RKKY interactions obtained in the weak-coupling limit. Rather than calculating the anisotropy in the Mn-Mn effective exchange within a microscopic model, we use a different approach to investigate the relevance of anisotropy for systems of diluted spins. We consider phenomenological models with disordered, anisotropic exchanges between classical Heisenberg spins placed randomly at low densities on a fcc lattice [corresponding to the Ga fcc sublattice in (Ga,Mn)As], and study the magnetic properties for several functional forms of the exchange interactions. This allows us to understand the effects modeled in each functional form separately, and thus assess their likely relevance to determining the magnetic properties of these materials. In each case we consider various values of the disorder and anisotropy. We focus on whether full saturation in magnetization is reached at low temperatures and also investigate the magnetic susceptibility, since this is known to be a good experimental indicator of spin freezing.⁹ Our results allow us to infer parameter ranges in which anisotropy and/or disorder are likely to play an important role in the magnetic properties of such systems.

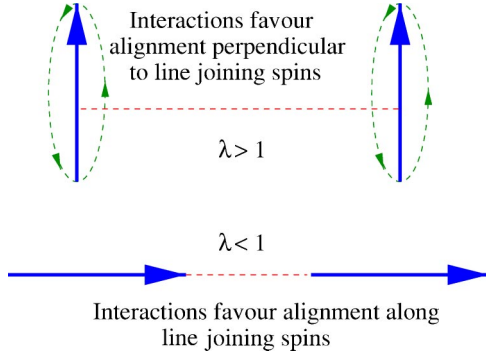


FIG. 1. Schematic representation of the two different types of anisotropy parametrized by λ . If $\lambda > 1$, the anisotropy defines an easy plane for the interactions between two spins, while if $\lambda < 1$ the anisotropy defines an easy axis.

The paper¹⁰ is organized as follows. In Sec. II we describe the models we study and how disorder and anisotropy are incorporated into each of them. Section III lists the quantities we calculate and how we perform the Monte Carlo simulations. Section IV shows our results for the magnetization, susceptibility, and Curie temperature and finally in Sec. V we discuss our results and their implications for modeling III-V DMS.

II. MODEL

We consider N_d spins randomly distributed at locations \mathbf{R}_i , $i = 1, \dots, N_d$ on a fcc lattice of size $N \times N \times N$, corresponding to an impurity concentration $x = N_d/4N^3$. The spins are treated as classical variables (Mn spins in $\text{Ga}_{1-x}\text{Mn}_x\text{As}$ have $S = 5/2$, so this is a reasonable approximation). For simplicity, we take the classical spins to have unit length; this is equivalent to rescaling the exchange from J to JS^2 , i.e.,

changing the units of energy. The most general formulation of the problem we consider in this study is provided by the Heisenberg Hamiltonian

$$\mathcal{H} = - \sum_{i,j} \sum_{\alpha\beta} J_{ij} F_{\alpha\beta}(\mathbf{R}_i - \mathbf{R}_j) S_i^\alpha S_j^\beta, \quad (1)$$

where α and β index Cartesian coordinates. The exchange coupling $J_{ij} F_{\alpha\beta}$ is written as a product of a random variable J_{ij} , and a function F of the separation of the two spins, for reasons that will become clear later. Since the sites are not on a regular lattice, the summation over site index is always over all sites of the system. For uncoupled spins i and j we simply have $F_{\alpha\beta}(\mathbf{R}_i - \mathbf{R}_j) = 0$. We consider the following parametrization of the exchange integral:

$$F_{\alpha\beta}(\mathbf{R}_i - \mathbf{R}_j) = [\lambda \delta_{\alpha\beta} + (1 - \lambda) \hat{e}_{ij}^\alpha \hat{e}_{ij}^\beta] f(r), \quad (2)$$

where $r = |\mathbf{R}_i - \mathbf{R}_j|$ and the unit vector $\hat{e}_{ij} = (\mathbf{R}_i - \mathbf{R}_j)/|\mathbf{R}_i - \mathbf{R}_j|$. The parameter λ controls the exchange anisotropy, and \mathbf{e}_{ij} defines the local axis of anisotropy for the pair of spins \mathbf{S}_i and \mathbf{S}_j located at \mathbf{R}_i and \mathbf{R}_j . Using Eq. (2), the effective interaction can now be rewritten as $J_{ij} S_i^\alpha F_{\alpha\beta}(\mathbf{R}_i - \mathbf{R}_j) S_j^\beta = J_{ij} f(r) (S_i^\parallel S_j^\parallel + \lambda S_i^\perp S_j^\perp)$, where the parallel and perpendicular components are defined with respect to \hat{e}_{ij} . As a result, for $\lambda = 1$ the model has no anisotropy and reduces to a simple disordered Heisenberg model. For $0 < \lambda < 1$ the couplings become anisotropic and favor alignment of each pair of spins along their axis \hat{e}_{ij} , while for $\lambda > 1$, the couplings favor alignment perpendicular to this axis (see Fig. 1). Since the relevant directions \hat{e}_{ij} differ considerably from pair to pair, frustration is introduced into the system, possibly leading to spin-glass physics.

The function $f(r)$ describes the spatial variation of the exchange interactions. In this work we investigate the following possibilities:

$$f(r) = \begin{cases} \theta(R_c - r), & \text{short-range FM, model A (Ref. 11)} \\ \frac{\sin y - y \cos y}{y^4}, & \text{RKKY, model B} \\ \frac{1}{r^4}, & \text{long-range FM, model C,} \end{cases} \quad (3)$$

where $y = 2k_F r$, and k_F is the Fermi wave vector. In the short-range model, equal-strength ferromagnetic interactions exist only between neighboring spins within distance R_c of one another.¹¹ The RKKY model allows interactions between all spins in the system, with oscillating sign depending on the Fermi wave vector k_F corresponding to different carrier concentrations. Finally we consider a purely ferromagnetic model with long-range (power-law) interaction. A comparison between the short-range and the long-range models clarifies

the role played by the *range* of the exchange, while a comparison between the RKKY and the long-range model clarifies the importance of the exchange *sign oscillations*.

In the RKKY approach of Zarand and Janko,¹ the relative magnitudes of the exchanges parallel, $K_{par}(r)$, and perpendicular, $K_{perp}(r)$, to the line joining two Mn spins depend on the distance r between the two spins. As a rough guide to compare with the models we study here, $|K_{perp}(r)| > |K_{par}(r)|$ for large r while $|K_{par}(r)| > |K_{perp}(r)|$ for small

r .⁸ It should be noted that we use the RKKY interaction for illustrative purposes only, since the exchange interactions in a more realistic model of DMS will likely be quantitatively different.

As demonstrated in mean-field and Monte Carlo studies of an impurity band model for III-V diluted magnetic semiconductors,^{8,12–19} and in studies of the kinetic-exchange model of III-V DMS including disorder and Coulomb interactions of the charge carrier with the Mn acceptors,²⁰ inhomogeneity induced by positional disorder of the Mn spins implies different local carrier charge densities at different sites, which in turn leads to a broad distribution of effective local fields created at various Mn sites by the itinerant carriers. If one integrates out the fermionic degrees of freedom and formulates the problem in terms of effective exchanges between the Mn spins, there should also be a wide distribution of their effective exchanges. To incorporate the effect of positional disorder leading to a wide distribution of magnitudes of the exchanges in our model, we assume that $J_{ij} = \epsilon_i \epsilon_j$, where the ϵ_i are random variables attached to each site, such that their logarithm $z_i = \log_{10} \epsilon_i$ has a Gaussian distribution

$$\mathcal{P}_{n_i}(z_i) = \frac{1}{\sqrt{2\pi}\sigma} \exp\left[-\frac{[z_i - z(n_i)]^2}{2\sigma^2}\right], \quad (4)$$

although the precise form of the disorder should not change our conclusions. In Eq. (4), the mean value $z(n_i)$ is taken to depend on the number n_i of nearest-neighbors spins (i.e., spins within a distance R_c) of the site i , through the relation $z(n_i) = \sigma(n_i - n_0)$, where n_0 is the average number of neighbors for a given cutoff R_c . In our simulations R_c is chosen such that $n_0 = 6$ or 12.

This scheme naturally favors stronger couplings within more dense clusters (higher n_i values) and hence should mimic some of the phenomenology observed in the impurity band model, where holes congregate in regions of higher Mn density leading to stronger effective interactions between the Mn in these regions.¹⁵ The parameter σ controls the width of the distribution of couplings, and thus characterizes the disorder present in the system; a more disordered system with a wider distribution of couplings corresponds to a larger value of σ .

Thus, the three parameters that control the behavior of the model are (i) λ , which controls the amount of anisotropy; (ii) σ , which controls the disorder-induced width of the distribution of effective exchanges; and (iii) R_c , which defines the average number of nearest neighbors for the short-range model (for the RKKY and long-range models, $R_c = \infty$).

III. SIMULATIONS

We performed exhaustive Monte Carlo simulations on each of models A , B , and C from above the ordering temperature T_c to well below T_c . We use a range of sizes to determine T_c via finite-size scaling, and average over a suf-

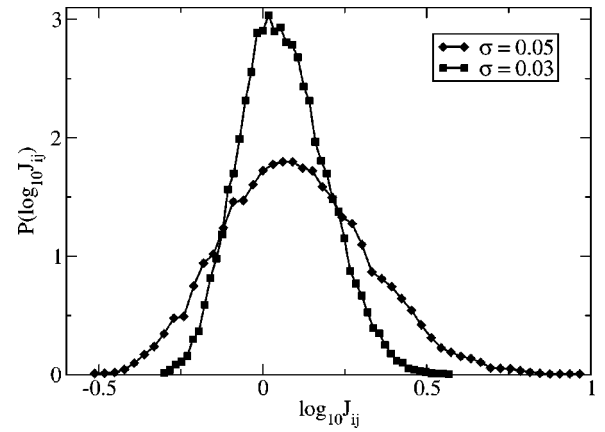


FIG. 2. Distribution of $\log_{10} J_{ij}$. Each curve is an average of five samples with $L = 32$, $N_d = 1310$, and $n_0 = 6$. The distribution is almost Gaussian, and its width increases with increasing σ .

ficient number of realizations of the disordered systems for each size to determine average quantities.

A. Parameters and calculated quantities

We investigated systems of linear sizes $L = 11, 14$, and 17, containing $N_d = 53, 110$, and 196 spins, respectively. This corresponds to a Mn density in $\text{Ga}_{1-x}\text{Mn}_x\text{As}$ of $x = 0.01$. The interaction range R_c is chosen such that the average number of nearest neighbors within R_c is either $n_0 = 6$, or $n_0 = 12$. We studied the short-range model for both values of n_0 . Note that for models with short-range interactions, the value of x has no *qualitative* effect on the behavior of magnetic properties for $x \leq 0.05$, since changing the concentration is equivalent to a pure rescaling of all interspin distances by a fixed factor. The value of x becomes relevant for larger concentrations, where the average interspin distance is comparable with the lattice constant. The anisotropy values considered were in the range $\lambda = 0.1$ to $\lambda = 10$, with the isotropic case $\lambda = 1$ used as a reference.

For the short-range model, two different disorder values were considered for most anisotropy values, while for the other models, only one disorder strength was considered. The values of σ considered were for short-range model, $\sigma = 0.017$ and 0.05 for $n_0 = 6$, and $\sigma = 0.01$ and 0.03 for $n_0 = 12$. For long-range model we chose $\sigma = 0.03$, while for the RKKY model, $\sigma = 0.01$. These values were chosen such that meaningful comparisons between different models can be performed, subject to some computational constraints. Figure 2 shows the actual distribution of J_{ij} used in the simulation for two different values of σ . For each pair of λ and σ values we considered many realizations of positional disorder of the Mn spins (generally at least 40) and averaged over these configurations to obtain our final results.

We calculated equilibrium (disorder averaged) averages for the following quantities: (i) the magnetization

$$M = \left\langle \frac{1}{N_d} \left| \sum_i \mathbf{S}_i \right| \right\rangle, \quad (5)$$

and (ii) the magnetic linear susceptibility

$$\chi_m = \beta \left(\left\langle \left| \frac{1}{N_d} \sum_i \mathbf{S}_i \right|^2 \right\rangle - M^2 \right). \quad (6)$$

To determine the Curie temperature in our samples we calculated the Binder cumulant

$$G(L, T) = \frac{1}{2} \left(5 - 3 \frac{\left\langle \left| \frac{1}{N_d} \sum_i \mathbf{S}_i \right|^4 \right\rangle}{\left\langle \left| \frac{1}{N_d} \sum_i \mathbf{S}_i \right|^2 \right\rangle^2} \right), \quad (7)$$

and used finite-size scaling. $G(L, T)$ is defined such that in the paramagnetic phase it decreases with L , $G \rightarrow 0$ as $L \rightarrow \infty$, while in the ferromagnetic phase it increases with L and tends to unity, $G \rightarrow 1$ as $L \rightarrow \infty$. Near T_c , this dimensionless quantity has the finite-size scaling form $G(L, T) = G[L^{1/\nu}(T - T_c)]$, where ν is the exponent of the diverging spin-spin correlation length $\xi \sim (T - T_c)^{-\nu}$.²¹⁻²³ At T_c , $G(L, T_c)$ is independent of L ; T_c can be identified by a simultaneous crossing of $G(L, T)$ versus T curves for different L . This method is found to be more reliable in determining T_c than the onset of magnetization, or the position of peaks in the magnetic susceptibility in relatively small finite-size samples.¹⁵

B. Temperature rescaling

In order to compare temperature scales for different λ values, we note that the effective exchange for a spin oriented at angle θ to the axis \mathbf{e}_{ij} is $J(\theta) = J_0 \sqrt{\cos^2 \theta + \lambda^2 \sin^2 \theta}$. Thus, $J_{\text{eff}}(\lambda) = 1/4\pi \int d\Omega J(\theta)$ gives the average exchange integrated over all solid angles Ω . Evaluating the integral gives²⁴

$$J_{\text{eff}}(\lambda) = J_0 \times \begin{cases} \frac{1}{2} \left[1 + \frac{\lambda^2}{\sqrt{\lambda^2 - 1}} \sin^{-1} \left(\frac{\sqrt{\lambda^2 - 1}}{\lambda} \right) \right], & \lambda > 1 \\ 1, & \lambda = 1 \\ \frac{1}{2} \left[1 + \frac{\lambda^2}{\sqrt{1 - \lambda^2}} \sinh^{-1} \left(\frac{\sqrt{1 - \lambda^2}}{\lambda} \right) \right], & \lambda < 1. \end{cases}$$

These factors are used to rescale the temperature for each value of λ chosen. We plot most quantities as a function of the rescaled temperature $k_B T / J_{\text{eff}}(\lambda)$.

C. Monte Carlo technique

The Metropolis algorithm necessitates long equilibration times at low temperatures and large values of anisotropy, due to its relatively slow sampling of the phase space. An efficient alternative is the continuous version of the heat-bath algorithm,²⁵ which was previously implemented for the classical Heisenberg ferromagnet^{25,26} and found to give values of the critical exponents of the ferromagnetic phase transition in agreement with other methods to high accuracy.²⁶ We find that the performance of the heat-bath method is superior to the Metropolis algorithm for the models we study here.

The continuous heat-bath algorithm can be used for any Hamiltonian \mathcal{H} that can be factorized as $\mathcal{H} = \sum_i \mathbf{h}_i \cdot \mathbf{S}_i$, where $\mathbf{h}_i = \sum_j J_{ij} \mathbf{S}_j$ is the local field created at site i by the other spins. In our model, \mathbf{h}_i contains terms of the form $\sum_j J_{ij} \mathbf{e}_{ij} (\mathbf{e}_{ij} \cdot \mathbf{S}_j)$. The implementation of a MC simulation requires successive spin flips at each site in the system for a MC step. Each spin flip involves changing the angular position vector of one spin, while keeping all others fixed. After a sufficiently large number of spin flips at each site, the angular distribution of these vectors will be equal to the equilibrium (Boltzmann) distribution. For any spin that is about to be flipped, the distribution of the angle θ between the spin and its local field \mathbf{h}_i (integrated over azimuthal angle) is

$$\rho(\theta) = \frac{k e^{k \cos \theta} \sin \theta}{e^k - e^{-k}}, \quad (8)$$

where $k = \beta |\mathbf{h}_i|$. The continuous heat-bath algorithm generates the random number θ by mapping a uniformly distributed random number $x \in [0, 1]$ to $\cos \theta \in [-1, 1]$ with a monotonic function $\cos \theta = f(x)$. The function $f(x)$ was derived in Ref. 25,

$$f(x) = 1 + \frac{1}{k} \ln [1 - x(1 - e^{-2k})]. \quad (9)$$

The calculation of k takes similar amounts of CPU time as evaluation of the energy difference in the usual Metropolis algorithm. The calculation of the mapping function $f(x)$ is more time consuming than a simple exponential function in the Metropolis algorithm, but it has the advantage of a 100% acceptance rate, while the Metropolis algorithm may have exponentially low acceptance rates. The evaluation of the mapping function can be optimized or tabulated to further increase the efficiency. After updating $\cos \theta$ we generate a random azimuthal orientation of the spin by randomly selecting a vector (of appropriate magnitude) perpendicular to the local field; this can also be done with a fast algorithm.

We compared the efficiency of both algorithms for our models. They produce the same equilibrium results, but the equilibration and autocorrelation times were found to be shorter by a factor of 10 to 100 depending on T and L , when using the continuous heat-bath algorithm for these models (see Fig. 3 for an illustration).

IV. RESULTS

We present the results we obtained for the magnetization for all three models. For the short-range model, we also present the susceptibility and the Curie temperature.

A. Short-range model

1. Magnetization

Our numerical simulations are for finite systems. To understand the extrapolation to the thermodynamic limit, we investigated the scaling of the magnetization $M(N_d, T)$ for systems with N_d spins at $T < T_c$, in the limit $N_d \rightarrow \infty$. A

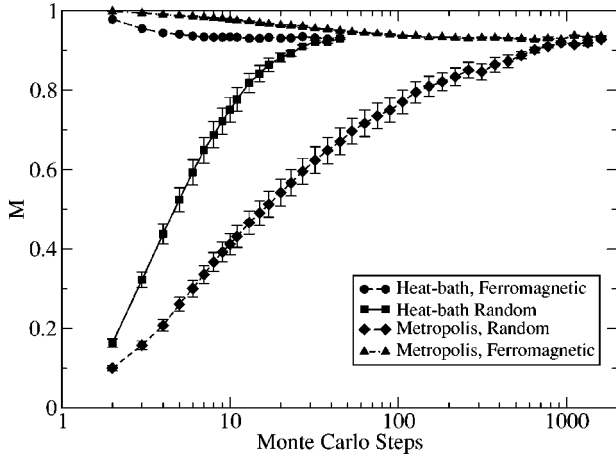


FIG. 3. A comparison of the Metropolis and the continuous heat-bath algorithms shows that convergence to equilibrium is accelerated about ten times by the latter. This simulation was done with $N_d=196$, $T=0.5$, $\lambda=0.5$, and $\sigma=0.1$. Equilibrium is determined by convergence between two replicas with different initial conditions, one with all spins aligned (ferromagnetic), and the other random. At lower T and for larger disorder, the heat-bath method reaches equilibration up to 100 times faster than the Metropolis algorithm.

typical result corresponding to the short-range model with $n_0=12$, $\lambda=0.5$ and for $T=1.3J_{\text{eff}}\sim 0.4T_c$ is shown in Fig. 4. Simulations for systems with up to $N_d=5000$ spins clearly demonstrate a finite value for $M(T)=\lim_{N_d\rightarrow\infty}M(N_d,T)$ for $T<T_c$, implying that these models have true ferromagnetic long-range order at low temperatures. Due to computational constraints, in the rest of this paper we show results from simulations with smaller numbers of spins N_d , for which proper disorder averages can be obtained in a reasonable amount of time.

The magnetization curves $M(T)$ shown in Fig. 5 for a size corresponding to $N_d=196$ spins have the characteristic linear decrease with temperature seen in previous work and in experiments in $\text{Ga}_{1-x}\text{Mn}_x\text{As}$.^{27,28} Comparison of Fig. 5(a) with

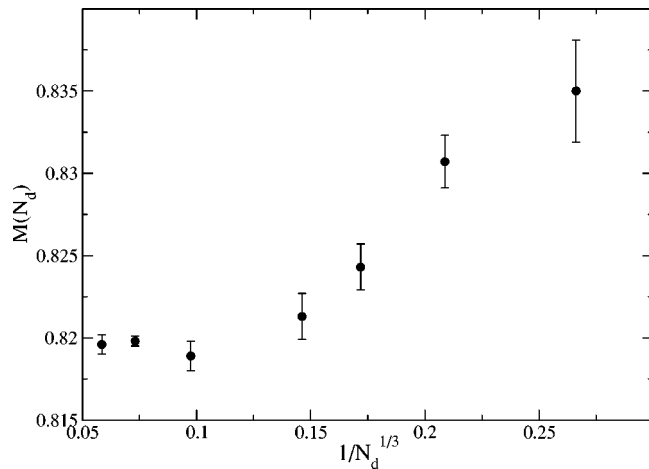


FIG. 4. Size dependence of the magnetization in the $n_0=12$ model for $\lambda=0.5$ at $T\sim 0.4T_c$.

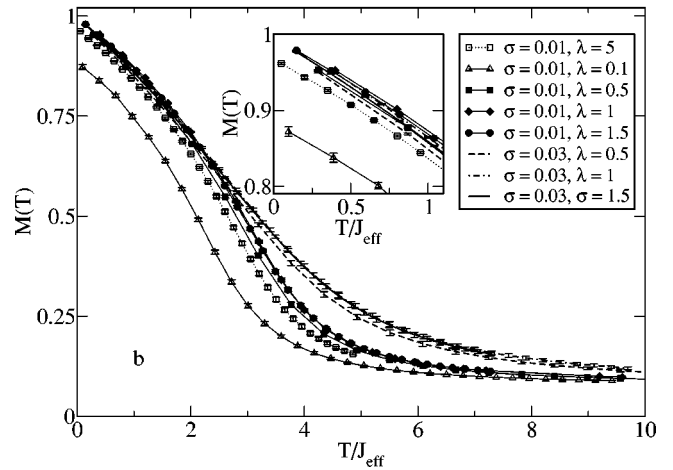
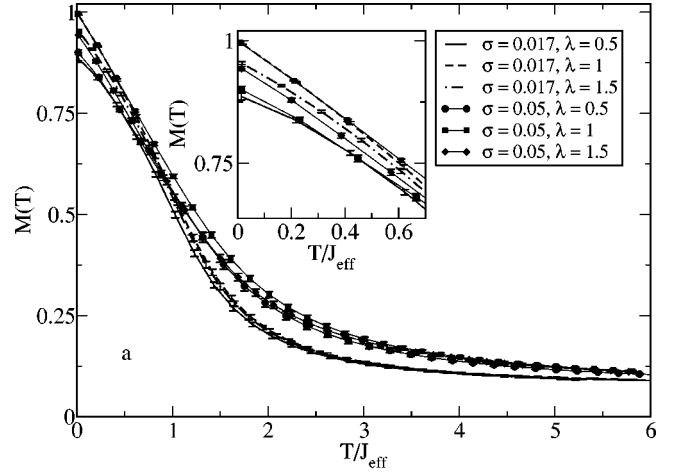


FIG. 5. Magnetization for (a) $n_0=6$ and (b) $n_0=12$, for various values of λ and σ . The simulations are for $N_d=196$ spins. The insets amplify the low-temperature regions.

Fig. 5(b) shows that increasing the number of nearest neighbors in the short-range model leads to a slightly more conventional *shape* for the magnetization curve. In both cases, $M(T)$ shows little curvature at low T , and a long tail at higher T . We also see from Fig. 5 that samples with $n_0=12$ have slightly increased curvature at low T . This is because the increased connectivity effectively reduces both spatial disorder and anisotropy, so that the samples show more conventional ferromagnetic features, as also seen from the results of susceptibility. This suggests that if we further increased the connectivity, we would likely see even more conventional $M(T)$ curves, as are found in samples subjected to postgrowth annealing^{3,4} where the hole concentration is increased significantly.²⁹

The roles of the anisotropy λ and disorder σ can also be inferred. We observe that curves corresponding to the same disorder value σ but various anisotropies λ are almost identical at high T . Increasing the disorder σ leads to increased magnetization at high T , as expected from studies of other models for DMS.^{13–15} Anisotropy plays a role at low T , where increased anisotropy does lower the $T=0$ magnetization, although the effect is rather small. The suppression is more pronounced for $\lambda<1$ (easy axis) than $\lambda>1$ (easy

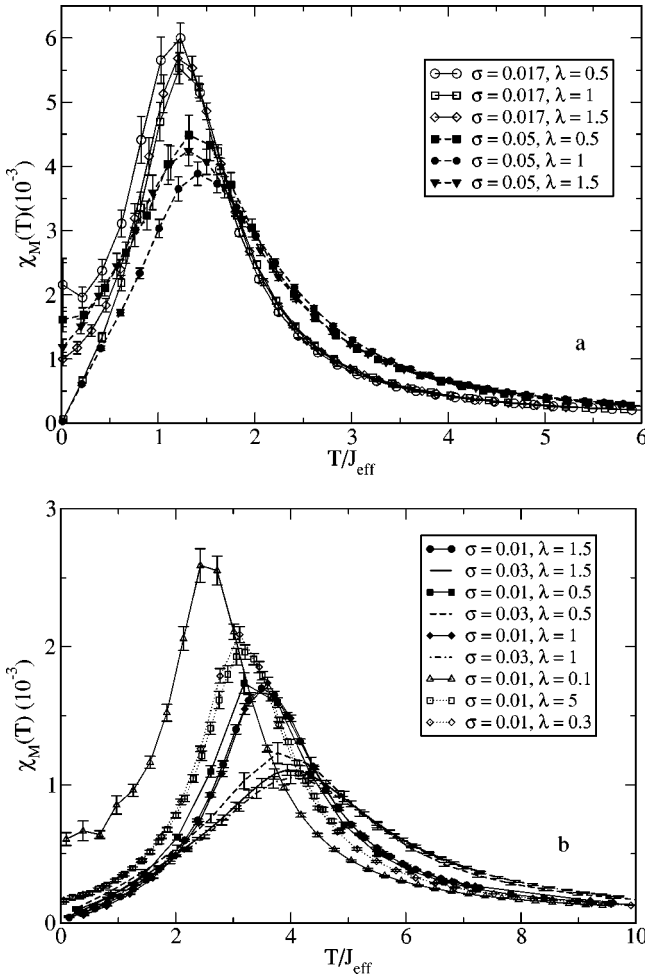


FIG. 6. Magnetic susceptibility for (a) $n_0=6$ and (b) $n_0=12$, with various values of λ and σ . The simulations are for $N_d=196$ spins.

plane). For $n_0=6$, the value of the saturation magnetization seems to depend only on λ and be independent of σ . For $n_0=12$, the suppression of low- T magnetization by anisotropy is rather weak except for an extremely large anisotropy $\lambda=0.1$. In the temperature range $T=0.1T_c \sim 0.5T_c$, both anisotropy and disorder effects affect the $M(T)$ curve.

2. Susceptibility

The behavior of the linear susceptibility for the short-range model with both 6 and 12 nearest neighbors is shown in Fig. 6. The high- T tails of the curves with the same disorder σ are again identical. At low T , anisotropy leads to a finite value for the $T=0$ linear susceptibility. The finite value of the linear susceptibility at $T=0$ is consistent with the incomplete saturation of magnetization in the presence of anisotropy. This effect is most transparent in the case of $n_0=6$; in contrast, for $n_0=12$, the effect of anisotropy is very weak unless the anisotropy is extreme, e.g., $\lambda > 5$ or $\lambda < 0.1$.

3. Curie temperature

The Curie temperatures are deduced from the Binder cumulant curves [see Eq. (7)]. Figure 7 shows curves calcu-

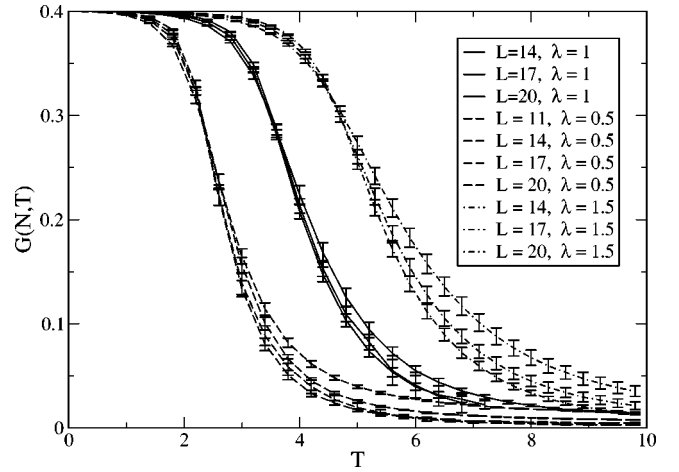


FIG. 7. Binder cumulant for models with 12 neighbors on average, $\sigma=0.01$, various anisotropy λ and sizes L .

lated for different system sizes for the 12 neighbor model. All curves corresponding to the same λ cross simultaneously, indicating the position of T_c . The system is ferromagnetic below T_c and paramagnetic above T_c . These critical temperatures are very close to the peaks in linear susceptibility of the same model, and are tabulated in Table I. Note that the temperature is not rescaled by J_{eff} in Fig. 7 in order to give a clear view of each set of curves. When the temperatures are rescaled as in Table I, the values of T_c are similar. This is expected, since all these curves correspond to the same disorder $\sigma=0.01$.

We conclude that small-to-moderate anisotropy has rather small effects on the low- T magnetic properties of the short-range model. Significant deviations from the isotropic behavior are seen only for very large values of the anisotropy, and are generally more pronounced in the $n_0=6$ model.

B. Long-range model

The qualitative behavior of the low- T magnetization in the long-range model is very similar to that observed in the short-range model, as can be seen in Fig. 8. Increasing the length scale of the exchange does very little to increase the amount of frustration in the model, and in both the short-range and the low-range model the suppression of the low- T magnetization is less than 20%, and often much smaller, for all values of anisotropy considered. This is small compared to the 50–60% reduction observed experimentally,⁶ hence other sources of frustration must be present to account for it. One candidate for the source of further reduction is the an-

TABLE I. Critical temperatures (in units of J_{eff} , see text) estimated from Binder cumulant $G(N,T)$ and magnetic susceptibility χ_M for $\sigma=0.01$ and $n_0=12$.

T_c/J_{eff}	From χ_M	From $G(N,T)$
$\lambda=0.5$	3.4 ± 0.2	3.4 ± 0.1
$\lambda=1$	3.6 ± 0.1	3.5 ± 0.1
$\lambda=1.5$	3.5 ± 0.1	3.4 ± 0.1

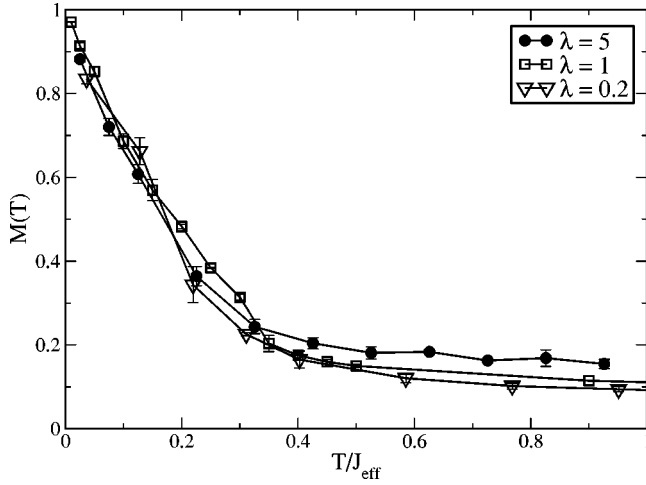


FIG. 8. Magnetization for $n_0=6$, various λ , $\sigma=0.03$, long-range model. In this case all pairs of spins interact, and n_0 is used only to adjust the average coupling constant.

tiferromagnetic component of effective Mn-Mn interactions as is found for RKKY interactions.

C. RKKY models

We calculated the magnetization for isotropic RKKY models with different Fermi wavelengths, corresponding to different charge-carrier concentrations. Our main observation is that the antiferromagnetic exchange at long distances introduced by the RKKY model has a significant effect on lowering the low- T magnetization; the decrease is considerably larger than that induced by anisotropy in both purely ferromagnetic models considered previously.

In Fig. 9 we show curves corresponding to several different values of the Mn concentration x and charge-carrier compensation $1-p$; the resulting charge-carrier concentration is $n_h=4xp/a^3$, where $a=5.65 \text{ \AA}$ is the GaAs lattice constant. Note that the temperature also needs to be rescaled by a factor of $(px)^{4/3}$ in three dimensions for RKKY

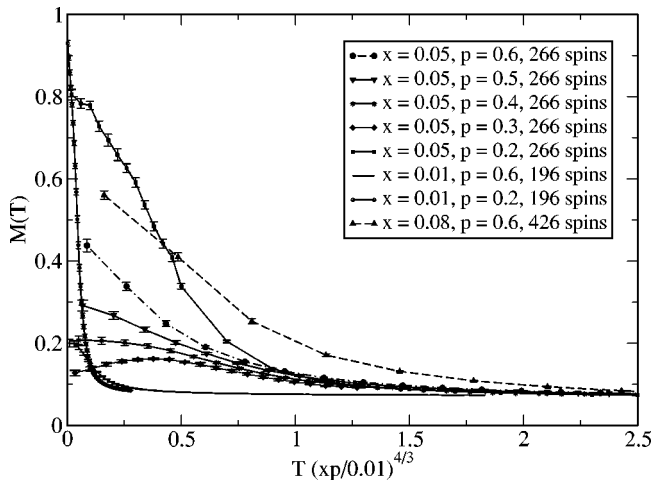


FIG. 9. Magnetization for the isotropic, $\lambda=1$ RKKY model, at various values of the Mn concentration x and hole compensation $1-p$ (corresponding to different choices of $y=2k_F r$).

interactions,³⁰ to meaningfully compare different magnetization curves. One interesting observation of the series with $x=0.05$ is that increasing the hole concentration px at fixed x does not appear to change T_c , but the low- T magnetization has a minimum at about $p=0.3$. Further increments of p increase the low- T magnetization gradually. There is a large range of values of the $T=0$ magnetization that can be achieved by tuning the Mn and the hole concentrations. This can be understood qualitatively in the following way: larger hole concentrations px lead to larger Fermi wave vectors k_F . As a result, the oscillation between ferromagnetic and antiferromagnetic interactions described by the RKKY interaction appears at a shorter distance. If this distance becomes comparable to the average interspin distance, significant frustration is present in the system leading to suppressed low- T magnetization. When $p=0.3$, the antiferromagnetic part seems to be dominant and the magnetization actually decreases as temperature is lowered below $0.4J_{\text{eff}}$. This effect arises due to antiferromagnetic coupling between clusters as a result of the long-range nature of the RKKY interaction.³¹ We have also investigated RKKY models with finite exchange anisotropy $\lambda \neq 1$. In all cases, the additional suppression of the low- T magnetization induced by the anisotropy is very small (less than 10%).

V. DISCUSSION

The major result that can be deduced from our simulations is that while exchange anisotropy can change the temperature scale at which ferromagnetism occurs in a model, it does not change the essential *qualitative* features such as the shape of the magnetization curve, or the form of the linear susceptibility greatly above T_c , unless the ratio between the parallel and perpendicular exchanges is extremely different from 1. Below T_c , the anisotropy preserves a finite magnetization and linear susceptibility at $T=0$. This effect is suppressed by higher connectivity (large n_0).³² In general, the effect of anisotropy is relatively weak, as it does not lower the magnetization at $T=0$ by more than 20%. The presence of antiferromagnetic interactions, as occur in oscillatory exchange interactions (e.g., the RKKY model) appears to be much more important for lowering the magnetization at low temperature. Thus the large reduction in the magnetization seen in Ref. 1 can probably be attributed to RKKY interactions, rather than the effects of anisotropy.

Our conclusion on the moderate effect of anisotropy on the magnetic properties of DMS is in substantial contrast with that of Zarand and Janko.¹ They found large differences between the low- T magnetization (but similar Curie temperatures) in the isotropic and anisotropic cases. We suggest that this difference may be due to their use of an exponential cutoff in the exchange interaction. The cutoff may have damped the effect of antiferromagnetic interactions in the isotropic case, but since the parallel and perpendicular exchanges had different spatial dependences in their study, its overall effect may be different in the isotropic and anisotropic cases.

There are a number of other interesting observations. The two types of anisotropy, corresponding to the cases $\lambda < 1$ and

$\lambda > 1$ are qualitatively different. For $\lambda < 1$, the spins preferentially align along the line joining them, while for $\lambda > 1$ there is a preferred plane in which the spins may lie. This difference in dimensionality appears to explain why the magnetization is not suppressed as much at low temperatures for $\lambda > 1$ as compared to $\lambda < 1$, since it is easier for spins to relax from frustration in two rather than one dimensions.

Anisotropic exchange interactions are just one of several possibilities which can lead to a reduction in the saturation magnetization in DMS at low T . First, there are antiferromagnetic nearest-neighbor interactions between Mn spins, which should have little effect due to the diluteness of the Mn spins, but could lead to a decrease in the saturation magnetization.³³ Next is a theoretical proposal that there is an instability purely in the presence of disorder towards a noncollinear ground state.^{2,34} Another is the experimental observation that there are significant numbers of interstitial Mn that appear to be involved in compensation processes and thus do not polarize.⁷ It is not completely clear to what extent the saturation at low temperatures in $\text{Ga}_{1-x}\text{Mn}_x\text{As}$ is due to nonparticipation of Mn spins *due to the presence of Mn interstitial defects*. However, given the recent progress in this area,⁷ it will probably not be long before an accurate estimate of the proportion of Mn that are participating in the ferromagnetism is known. When this is quantified, it should be possible to determine whether anisotropy needs to be included in realistic models of DMS. The carrier-mediated nature of the ferromagnetism also suggests that anisotropy may be important for transport, especially in the insulating phase, since hopping between sites will be preferred when the Mn spins have similar orientations.³⁵

We mention in passing that while anisotropy has a small

effect on the magnetization, it seems to have significant effect on the nonlinear susceptibility at low temperature.³⁶ This suggests that experimental investigations of the nonlinear susceptibility might shed light on the magnetic state in DMS. It was recently suggested that for $x < 0.01$ and $x > 0.1$ in $\text{Ga}_{1-x}\text{Mn}_x\text{As}$, there may be a spin glass phase.³³ Here we suggest that if there are strongly anisotropic exchange interactions, the ferromagnetic phase below T_c might have unconventional properties. Signatures of spin-glass behavior might be seen in coexistence with ferromagnetism. If such spin-glass signatures are not seen in $(\text{Ga},\text{Mn})\text{As}$, they may be present in other insulating materials with lower carrier concentrations such as $\text{Ge}:\text{Mn}$.³⁷

In conclusion, there are still a number of outstanding questions as to the nature of the ferromagnetic state in DMS, and whether anisotropy plays an important role in these materials. This work should be of help in clarifying which types of models are likely to be affected by anisotropy and what types of experimental probes might help to detect it.

ACKNOWLEDGMENTS

We thank Gergely Zarand for stimulating conversations, Chris Henley for insightful comments, and the Princeton Computer Science department for access to some of their computing resources. This research was supported by NSF, Grants Nos. DMR-9809483 and 0213706 (C.Z., M.P.K., M.B., R.N.B.) and DMR-9971541 (X.W.). X.W. acknowledges support from the State of Florida. M.B. acknowledges support from NSERC. X.W., M.B., and R.N.B. also thank the Aspen Institute for Physics for hospitality while parts of this work were carried out.

*Present address: Institut für Nanotechnologie, Forschungszentrum Karlsruhe, D-76021 Karlsruhe, Germany.

¹G. Zarand and B. Janko, Phys. Rev. Lett. **89**, 047201 (2002).

²J. Schliemann and A.H. MacDonald, Phys. Rev. Lett. **88**, 137201 (2002).

³S.J. Potashnik, K.C. Ku, S.H. Chun, J.J. Berry, N. Samarth, and P. Schiffer, Appl. Phys. Lett. **79**, 1495 (2001).

⁴K.W. Edmonds, K.Y. Wang, R.P. Campion, A.C. Neumann, N.R.S. Farley, B.L. Gallagher, and C.T. Foxon, Appl. Phys. Lett. **81**, 4991 (2002); K.C. Ku, S.J. Potashnik, R.F. Wang, S.H. Chun, P. Schiffer, N. Samarth, M.J. Seong, A. Mascarenhas, E. Johnston-Halperin, R.C. Myers, A.C. Gossard, and D.D. Awschalom, *ibid.* **82**, 2302 (2003).

⁵N. Theodoropoulou, A.F. Hebard, S.N.G. Chu, M.E. Overberg, C.R. Abernathy, S.J. Pearton, and R.G. Wilson, Appl. Phys. Lett. **79**, 3542 (2001); N. Theodoropoulou, K.P. Lee, M.E. Overberg, S.N.G. Chu, A.F. Hebard, C.R. Abernathy, S.J. Pearton, and R.G. Wilson, J. Nanosci. Nanotechnol. **1**, 101 (2001); K. Sato, G.A. Medvedkin, T. Nishi, Y. Hasegawa, R. Misawa, K. Hirose, and T. Ishibashi, J. Appl. Phys. **89**, 7027 (2001).

⁶A. Oiwa, S. Katsumoto, A. Endo, M. Hirasawa, Y. Iye, H. Ohno, F. Matsukura, A. Shen, and Y. Suguwara, Solid State Commun. **103**, 209 (1997).

⁷K.M. Yu, W. Walukiewicz, T. Wojtowicz, I. Kuryliszyn, X. Liu, Y. Sasaki, and J.K. Furdyna, Phys. Rev. B **65**, 201303(R) (2002).

⁸G.A. Fiete, G. Zarand, and K. Damle, Phys. Rev. Lett. **91**, 097202 (2003); for more precise treatments see L. Brey and G. Gómez-Santos, Phys. Rev. B **68**, 115206 (2003).

⁹R. Omari, J.J. Prejean, and J. Souletie, J. Phys. (France) **44**, 1069 (1983).

¹⁰Preliminary versions of this work was presented at the MRS meeting, Boston, 2002 and APS March meeting, Austin, TX, 2003. (The abstract can be found at <http://www.aps.org/meet/MAR03/baps/abs/S7910014.html>)

¹¹To be more precise, each spin is coupled to at least two other neighboring spins. If a spin has less than two neighbors within a distance R_c , then we assume it to be coupled to its two closest neighbors (irrespective of how far they are). This avoids the existence of completely isolated spins in our model. For the values of R_c we investigate, we find that only about 1–2 % of spins are in this situation.

¹²M.P. Kennett, M. Berciu, and R.N. Bhatt, Phys. Rev. B **65**, 115308 (2002).

¹³M. Berciu and R.N. Bhatt, Phys. Rev. Lett. **87**, 107203 (2001).

¹⁴M. Berciu and R.N. Bhatt, Phys. Rev. B **69**, 045202 (2004).

¹⁵M.P. Kennett, M. Berciu, and R.N. Bhatt, Phys. Rev. B **66**, 045207 (2002).

¹⁶R.N. Bhatt, M. Berciu, M.P. Kennett, and X. Wan, J. Supercond. **15**, 71 (2002).

¹⁷R.N. Bhatt, X. Wan, M.P. Kennett, and M. Berciu, Comput. Phys. Commun. **147**, 684 (2002).

- ¹⁸M. Mayr, G. Alvarez, and E. Dagotto, Phys. Rev. B **65**, 241202(R) (2002); G. Alvarez and E. Dagotto, *ibid.* **68**, 045202 (2003).
- ¹⁹M.J. Calderón, G. Gómez-Santos, and L. Brey, Phys. Rev. B **66**, 075218 (2002).
- ²⁰S.-R. Eric Yang and A.H. MacDonald, Phys. Rev. B **67**, 155202 (2003).
- ²¹K. Binder and A.P. Young, Rev. Mod. Phys. **58**, 801 (1986).
- ²²R.N. Bhatt and X. Wan, Int. J. Mod. Phys. C **10**, 1459 (1999).
- ²³X. Wan and R.N. Bhatt, cond-mat/0009161 (unpublished).
- ²⁴I. S. Gradshteyn and I. M. Ryzhik, *Table of Integrals, Series and Products*, 5th ed., edited by A. Jeffrey (Academic Press, London, 1994).
- ²⁵Y. Miyatake, M. Yamamoto, J.J. Kim, M. Toyonaga, and O. Nagai, J. Phys. C **19**, 2539 (1986).
- ²⁶R.G. Brown and M. Ciftan, Phys. Rev. Lett. **76**, 1352 (1996).
- ²⁷B. Beschoten, P.A. Crowell, I. Malajovich, D.D. Awschalom, F. Matsukura, A. Shen, and H. Ohno, Phys. Rev. Lett. **83**, 3073 (1999).
- ²⁸H. Ohno and F. Matsukura, Solid State Commun. **117**, 179 (2001).
- ²⁹Increasing the hole concentration effectively corresponds to increasing the connectivity in our model.
- ³⁰T. Dietl, J. Cibert, D. Ferrand, and Y.M. d'Aubigne, Mater. Sci. Eng., B **63**, 103 (1999).
- ³¹D.J. Priour, E.H. Hwang, and S. Das Sarma, Phys. Rev. Lett. **92**, 117201 (2004).
- ³²Locally the random lattice with $n_0=12$ is more symmetric than for $n_0=6$, so the anisotropy a spin feels from one neighbor is more likely to be canceled by the effects of other neighbors.
- ³³S. Das Sarma, E.H. Hwang, and A. Kaminski, Phys. Rev. B **67**, 155201 (2003).
- ³⁴A.L. Chudnovskiy and D. Pfannkuche, Phys. Rev. B **65**, 165216 (2002).
- ³⁵A.A. Burkov and L. Balents, Phys. Rev. Lett. **91**, 057202 (2003).
- ³⁶M. P. Kennett, C. Zhou, X. Wan, M. Berciu, and R. N. Bhatt (unpublished).
- ³⁷S. Cho, S. Choi, S.C. Hong, Y. Kim, J.B. Ketterson, B.J. Kim, Y.C. Kim, and J.H. Jung, Phys. Rev. B **66**, 033303 (2002).